JOURNAL OF SOLID STATE CHEMISTRY 56, 191–202 (1985)

A Kinetic Study on the Reaction of Hydrogen with Mg_2Ni

M. Y. SONG, M. PEZAT, B. DARRIET, AND P. HAGENMULLER

Laboratoire de Chimie du Solide du CNRS, Université de Bordeaux I, 351, cours de la Libération—33405 Talence Cedex, France

Received February 8, 1984; in revised form July 23, 1984

The kinetics of the reaction of hydrogen with Mg_2Ni has been investigated under hydrogen pressures from 3 up to 7 bar at various temperatures ($548 \leq T \leq 593$ K). Hydrogen absorption rates for the hydriding reaction show an inverse temperature dependence under our experimental conditions. The results are analyzed by considering the increase in temperature due to the heat of reaction in the course of hydrogen absorption. The rate-controlling step for hydriding reaction in the initial stage is the dissociative chemisorption on Ni involving heat transfer as "a rate-delaying step." In later stages, hydrogen absorption rates decrease gradually with the effect of the particle size distribution and the diminution of the unreacted fraction. Other phenomena are also discussed, i.e., hydrogen absorption in α-solid solution region and an incubation period. © 1985 Academic Press, Inc.

Introduction

Mg_2Ni is considered as an appropriate material for hydrogen storage from the viewpoint of hydrogen storage capacity (about 3.7 wt%), hydride stability (*1*, *2*), and hydriding kinetics.

Hydriding kinetics is basic to an understanding of the hydriding reaction mechanisms. However, very few studies have been reported on the hydriding kinetics of the Mg_2Ni–H_2 system (*3–6*).

Seiler *et al.* (*7*) reported that a small amount of oxygen induces a surface segregation, leading to an overlayer of oxidized magnesium and leaving behind at least some nickel in the metallic state. This segregated nickel can act as a set of active sites for the dissociative chemisorption of hydrogen (*8*).

With these results the hydriding process of the activated Mg_2Ni can be classified as follows (*9–11*):

(1) Mass transport of H_2 molecules up to the surface of Mg_2Ni or Ni.

(2) Dissociative chemisorption of H_2 molecules on the surface of Mg_2Ni or Ni.

(3) For hydrogen atoms chemisorbed on the surface of Ni: (a) the surface diffusion of hydrogen atoms on the Ni surface to the grain boundary of nickel and magnesium oxide; (b) the diffusion of hydrogen atoms through the grain boundaries between nickel and magnesium oxide.

(4) Transition of hydrogen atoms from their chemisorbed state into their absorbed state.

(5) Diffusion of hydrogen atoms through the growing layer of hydride.

(6) Phase transformation (α-solid solution of hydrogen in $Mg_2Ni \rightarrow$ hydride).

In addition heat transfer may also be an important step for hydriding. The increase in temperature during the reaction decreases the hydrogen absorption rates by raising the equilibrium plateau pressure

0022-4596/85 $3.00

(P_{eq}) and causing a diminuation of the driving force ($P_0 - P_{eq}$) for hydriding, P_0 being the hydrogen pressure.

The rate-controlling step for hydriding Mg_2Ni has been determined. Other phenomena related to hydrogen absorption by Mg_2Ni are also discussed.

Experimental

Sample preparation. A mixture of powders of Mg (Ventron, 50 mesh, 99,8% purity) and nickel (Cerac, 325 mesh, 99,9% purity) in the proportions corresponding to the composition $Mg_{2.05}Ni$ was pressed under 3 tons/cm^2 during 2 min. This composition was chosen as during the reaction a small quantity of Mg is evaporated. Then the pellet was sintered under an argon atmosphere of 3 bar at 823 K during about 120 hr in a stainless-steel crucible. Sintering was used rather than melting due to the necessity of controlling the Mg_2Ni composition; during melting too much Mg evaporates. In these conditions every time a small quantity of MgO was found present by X-ray analysis. In addition a magnetic measurement showed an excess of Ni of about 2.7 wt% which could not form Mg_2Ni because of Mg evaporation and of the experimental conditions.

Apparatus. Figure 1 schematically represents the hydriding set made of stainless steel. It consists of three parts: A: purification of hydrogen; B: standard volume; C: reactor. Part A is filled with Mg chips maintained at 823 K to dry and deoxygenate the supplied hydrogen (AIR LIQUIDE, U quality). Part B includes a standard volume, linked to a Bourdon gauge M_2 which permits measuring the pressure from 0 to 10 bar with a precision of 0.05 bar. Part C consists of a Bourdon gauge M_1, identical with M_2, connected to the reactor by a capillary tube (internal diameter ≈ 4 mm). The thermocouple is located within the wall of the reactor. Separate tests have shown that there is very little difference in temperature readings and only a small time lag between a thermocouple located at the sample loca-

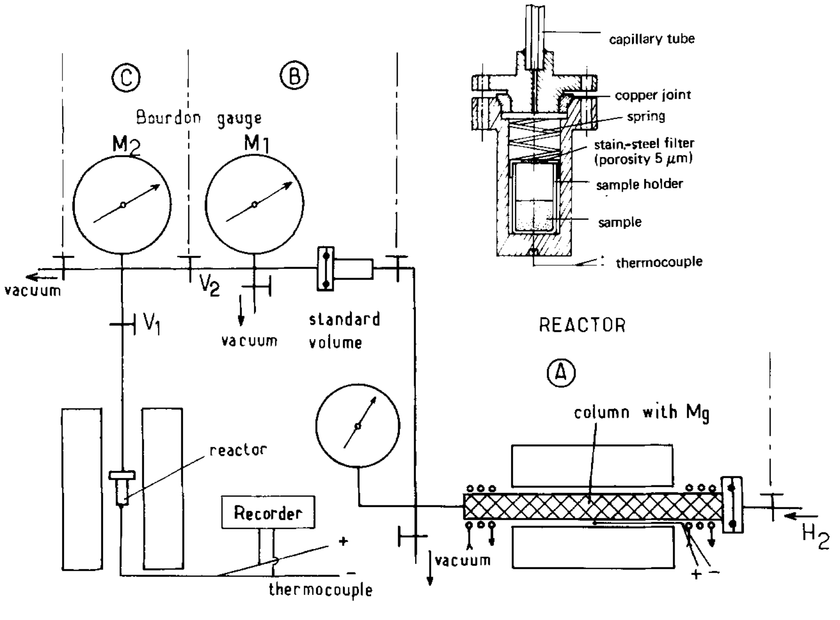

FIG. 1. Scheme of the apparatus for hydrogenation.

tion and that within the reactor walls. The changes in the temperature were recorded. The dead volumes of parts B and C are 64.9 and 58.5 cm^3, respectively. For the study of hydrogen absorption under pressures higher than 10 bar a similar apparatus was used.

Determination of the quantity of absorbed hydrogen as a function of time. The amount of used Mg_2Ni was about 1.1 g. The particle size crushed in air was less than 200 μm. The hydrogen pressure were maintained nearly constant during the reaction by employing appropriate dosing volumes. The fall of pressure was 1 ~ 5% of the chosen pressure in the course of our measurements. The variation of the pressure of hydrogen in the known volume of B permits one to calculate the quantity of hydrogen absorbed by the sample as a function of time. The activation was carried out under the hydrogen of 7 bar at 573 K. It was completed after 7 cycles. The hydrogen absorption rates are measured under hydrogen pressures from 3 up to 7 bar, between 548 and 593 K.

Results and Analyses

We define the reacted fraction F as follows: $F \equiv$ number of H_2 moles absorbed during t minutes/number of H_2 moles calculated on the assumption that 100% of the activated sample is hydrided into the composition Mg_2NiH_4.

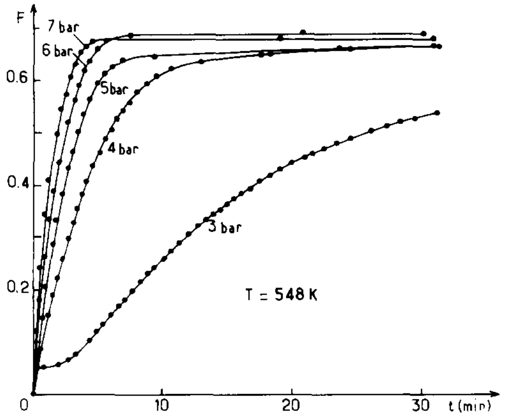

FIG. 2. Influence of hydrogen pressure on the hydrogenation of the activated Mg_2Ni powder at 548 K between 34th and 39th hydriding cycles.

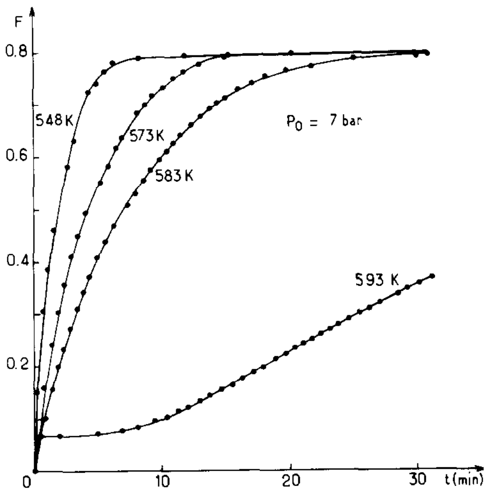

FIG. 3. Influence of temperature on the hydrogenation of the activated Mg_2Ni powder under hydrogen pressure of 7 bar between 10th and 13th hydriding cycles.

Figure 2 shows the influence of hydrogen pressure (P_0) on the hydrogen absorption by the activated Mg_2Ni powder at a constant temperature ($T = 548$ K) between the 34th and 39th hydriding cycles.

Figure 3 shows the influence of temperature on the hydrogen absorption of the alloy under constant hydrogen pressure ($P_0 = 7$ bar) between the 10th and 13th hydriding cycles.

The F–t curves for $P_0 = 3$ bar of Fig. 2 and $T = 593$ K of Fig. 3 exhibit (at the very beginning) a very rapid initial hydrogen absorption up to $F \simeq 0.053$ and $\simeq 0.065$, respectively. Then they show an incubation period of 2 and 7 min approximately.

Figure 4 shows the initial parts of some F–t curves scaled up. The region from $F = 0$ to the points S (Region I in Fig. 4) is thought to correspond to a nonsaturated α-solid solution, and to an extremely small amount of surface hydride of Mg_2Ni. This point will be explained in the discussion section.

After these initial periods, the actual hydriding reaction begins (Region II of Fig. 4). Our main interest is devoted here to Region II.

The F–t curves of Figs. 2, 3, and 4 show a linear behavior in the initial stage of the hydriding reaction (stage A), but their slopes decrease gradually in a later stage (stage B).

By transmission electron micrographs the activated Mg_2Ni particles are observed to have irregular shapes and various sizes. In the initial stage of the hydriding reaction, almost all the particles are considered to have an unreacted fraction and to participate in the reaction. There would be a small change in the reaction interface area even if the reaction interface advances. Therefore, the real reaction rates can be obtained from the initial stage of the hydriding reaction rather than from the later stage.

A. Initial Stage of the Hydriding Reaction (Region II)

A-1. The Dependence of the Hydriding Reaction Rates on the Hydrogen Pressures (P_0)

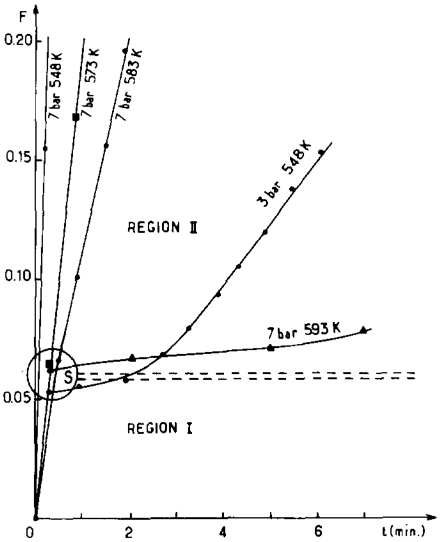

FIG. 4. Initial parts of the F–t curves of Figs. 2 and 3.

From the slopes of the F–t curves (Fig. 2) in the initial stage of the hydriding reaction ($\sim 0.05 \leq F \leq \sim 0.40$), the hydriding reaction rates dF/dt (min^{-1}) are deduced. They are listed in Table I, where F^* is the reacted fraction when $t = t^*$ (t^* is the time at which an appreciable hydriding reaction begins to take place).

TABLE I

HYDRIDING REACTION RATES dF/dt UNDER VARIOUS HYDROGEN PRESSURES IN THE RANGE $\sim 0.05 \leq F \leq \sim 0.40$ AT 548 K

P_0 (bars)	$\frac{dF}{dt} \times 10$ (min^{-1})	F^*	t^* (min)
3	0.28	0.093	3.88
4	0.98	0.049	0.17
5	1.67	0.063	0.28
6	2.10	0.087	0.15
7	2.80	0.121	0.15

Figure 5 shows that the hydriding reac-

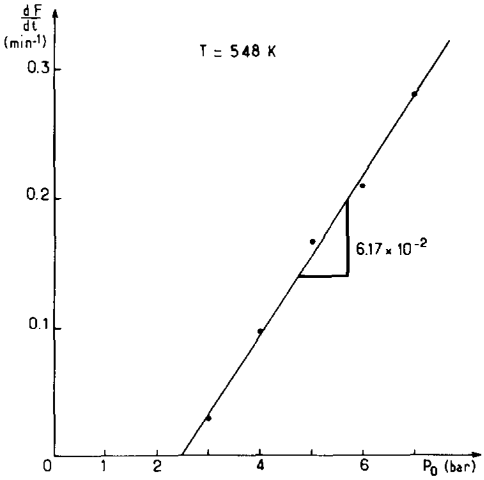

FIG. 5. Dependence of the hydriding reaction rates on the hydrogen pressures.

tion rates vary linearly with the hydrogen pressures, i.e.,

$$\frac{dF}{dt} = aP_0 + b, \quad (2)$$

where a and b are constants at a given temperature.

Since $dF/dt = 0$ when $P_0 = P_{eq}$ (P_{eq} is the equilibrium plateau pressure at a given temperature), Eq. (2) can be rewritten as

$$\frac{dF}{dt} = a(P_0 - P_{eq}). \quad (3)$$

The relation between dF/dt and P_0 obtained at 548 K (Fig. 5) is

$$\frac{dF}{dt} = 6.17 \times 10^{-2}[P_0(\text{bar}) - 2.46]. \quad (4)$$

In the initial stage of the hydriding reaction, an increase in the temperature 4.3–5.5 K was detected, which varies with hydrogen pressures and temperatures. To simplify the analyses, it is assumed that at all experimental conditions, the increase in temperature is 5 K which is approximately the average value of 4.3 and 5.5 K. This assumption is not considered as causing very significant errors in the analyses of the hydriding process.

The reported data of the equilibrium plateau pressures for hydrogen absorption at 548 and 553 K are 2.27 and 2.45 bar, respectively (4). The equilibrium plateau pressure of 553 K is in excellent accord with the value of 2.46 bar which is obtained by comparing Eq. (4) with Eq. (3). This indicates that Eq. (3) is quite relevant, i.e., that the hydriding reaction rates show a linear dependence on the hydriding driving force ($P_0 - P_{eq}$). The proportionality constant, a, depends on the temperature.

A-2. The Dependence of the Hydriding Reaction Rates on Temperature

From the slopes of the F–t curves (Fig. 3) in the initial stage of the hydriding reaction the hydriding rates dF/dt (min^{-1}) are obtained. They are listed in Table II.

TABLE II

HYDRIDING REACTION RATES dF/dt AT VARIOUS TEMPERATURES IN THE RANGE $\sim 0.05 \leq F \leq \sim 0.40$ UNDER CONSTANT HYDROGEN PRESSURE OF 7 BAR

T (K)	$\frac{dF}{dt} \times 10$ (min^{-1})	F^*	t^* (min)
548	2.59	0.095	0
573	1.47	0.063	0.22
583	0.86	0.066	0.48
593	0.13	0.097	9.45

The hydriding reaction rates decrease strongly with increasing temperature. This can be considered as being due primarily to the decrease of the driving force for hydriding, ($P_0 - P_{eq}$), with increasing temperature.

If the temperature dependence of the hydriding reaction rates is expressed by an Arrhenius law, Eq. (3) can be written as

$$\frac{dF}{dt} = A_1(P_0 - P_{eq}) \exp\left(-\frac{E_1}{RT}\right), \quad (5)$$

where A_1 is the preexponential factor and E_1, the apparent activation energy for the reaction. By using the hydriding reaction rates of Table II, A_1 and E_1 of Eq. (5) are calculated with a least-square method, and represented by a straight line A in Fig. 6, where $\ln[(dF/dt)/(P_0 - P_{eq})]$ vs $1/T$ is plotted. For the equilibrium plateau pressure (P_{eq}) for absorption, the data of Nomura *et al.* (*4*) have been employed

$$\log_{10} P_{eq}(\text{bar}) = -3.245/T + 6.2558. \quad (6)$$

The plot actually is not really linear. An apparent activation energy E_1 is $-15{,}500$ cal/mole H_2 (Eq. (7)) is obtained, so that

$$\frac{dF}{dt} = 4.37 \times 10^{-8}(P_0 - P_{eq}) \exp\left[\frac{15{,}500(\text{cal/mole } H_2)}{RT}\right]. \quad (7)$$

The negative value of that activation energy reflects that a nonthermally activated process, namely heat transfer, is a rate-controlling step.

As far as heat transfer is concerned, a "rate-delaying" step is preferable to a rate-controlling one, since an increase in temperature retards the hydriding reaction rates by decreasing the driving force ($P_0 - P_{eq}$). The observed increase in temperature in the course of the hydriding reaction proves that heat transfer is actually a "rate-delaying step." The poor linearity in the Arrhenius-type plot suggests that there is another rate-controlling step in addition to heat transfer.

To analyze more closely the intrinsic chemical reaction mechanism, the influence of the heat transfer must be eliminated.

In Fig. 6, line B represents the plot of $\ln[(dF/dt)/(P_0 - P_{eq})]$ vs $1/T$ by considering an increase in temperature of 5 K. This exhibits relatively good linearity, but again an apparent activation energy of −350 cal/mole H_2 which is negative (Eq. (8)).

$$\frac{dF}{dt} = 4.14 \times 10^{-2}(P_0 - P_{eq}) \exp\left[\frac{350(\text{cal/mole H}_2)}{RT}\right]. \quad (8)$$

The fact that the apparent activation energy is still negative, in spite of the consideration of an temperature increase of 5 K due to heat transfer, suggests that (i) either the increase in temperature is larger than 5 K; (ii) or there is another rate controlling step which is responsible for the inverse temperature dependence in this temperature range. The relatively good linearity in the Arrhenius-type plot indicates that the small value found for the apparent activation energy is valid. Of course, the rate equation for this step must satisfy the dependence of pressure, i.e., be a first-order function of ($P_0 - P_{eq}$) (see Eq. (3)).

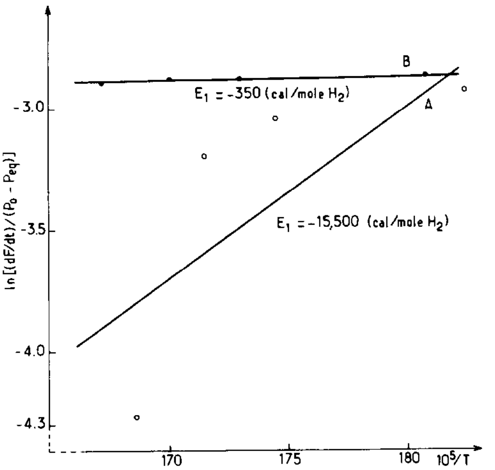

FIG. 6. Arrhenius-type plot of $\ln|(dF/dt)/(P_0 - P_{eq})|$ vs $1/T$. (A) Not considered the increase in temperature, (B) considered an increase in temperature of 5 K.

Incidentally, if the increase in temperature were greater than 5 K, the driving force for hydriding ($P_0 - P_{eq}$) would be nearly zero or negative, causing the reaction to be stopped or at least, to be extremely slow. We also note that the inverse temperature dependence is likewise observed at 522 and 571 K under the constant hydrogen pressure of 30 bar where ($P_0 - P_{eq}$) is about 28.9 and 26.3 bar, repectively. While in those examples the difference in the driving forces for hydriding is negligible, that of temperature is large. The fact that despite such experimental conditions the hydriding rates show an inverse temperature dependence shows clearly that *this inverse temperature relation is a real trend in the hydriding reaction of* Mg_2Ni.

This suggests that hypothesis (ii) is applicable.

A powerful candidate for the requirements of the inverse temperature dependence and the negligible activation energy is indeed the dissociative chemisorption of hydrogen on the metal surface (*12–14*). Let us consider now the overall rate equation if we suppose that this step is rate controlling.

Beeck (*15*), Anderson and Baker (*16*) found that each atom of nickel on the surface takes up one atom of hydrogen. Thus the dissociative chemisorption of hydrogen can be expressed as

$$H_2 + 2|S \underset{k_b}{\overset{k_f}{\rightleftharpoons}} 2(|S\text{–}H) \tag{9}$$

where $|S$ is the surface active site of Ni or Mg$_2$Ni, k_f and k_b being the rate constants for the forward and backward reactions, respectively.

Ideally we must begin to measure the hydriding reaction rates after the terminal solubility of hydrogen into the activated Mg$_2$Ni is reached, which is the concentration at which the hydride starts to precipitate, and where the chemisorption of hydrogen is at equilibrium under the hydrogen pressure of P_{eq}.

The behavior of the F–t curves observed in the region of the hydriding reaction of Figs. 2 and 3, however, was observed to be exactly the same as that of the F–t curves obtained after hydrogen saturation up to the terminal solubility. Thus, even if we do not use the ideal experimental conditions described above in order to analyze the hydriding reaction, it cannot be considered to be a source of significant error.

If θ_{eq} is an equilibrium coverage under P_{eq} at a given temperature, the chemisorption rate ν is given by Eq. (10) with a steady-state approximation when hydrogen pressure is P_0 (*17, 18*):

$$\nu = k_f(1 - \theta_{eq})^2 P_0 - k_b\theta_{eq}^2. \tag{10}$$

In the hydriding reaction, when the hydrogen pressure P_0 becomes equal to the equilibrium plateau pressure P_{eq}, the driving force for hydriding is zero, leading the chemisorption rate $\nu = 0$. Thus, Eq. (10) can be written as

$$\nu = k_f(1 - \theta_{eq})^2(P_0 - P_{eq}). \tag{11}$$

From the kinetic theory of gases, the flux of adsorption ν_1 is given by ((*13*), p. 105 in (*17*))

$$\nu_1 = \frac{\sigma P_0}{(2\pi mkT)^{1/2}}(1 - \theta_{eq})^2 \exp\left(-\frac{E_a}{RT}\right), \tag{12}$$

where σ is a steric factor or a condensation coefficient defined as the fraction of the total number of colliding molecules possessing the necessary activation energy E_a for resulting in adsorption, $P/(2\pi mkT)^{1/2}$ is the number of molecules of mass m striking unit area of surface in unit time and k Boltzmann constant.

The flux ν_{-1} of desorption can likewise be written as

$$\nu_{-1} = k_{-1}\theta_{eq}^2 \exp\left(-\frac{E_d}{RT}\right), \tag{13}$$

where k_{-1} is the specific rate constant for desorption and E_d stands for the activation energy of desorption. Therefore the net chemisorption rate ν is given by

$$\begin{aligned}\nu &= \nu_1 - \nu_{-1}\\ &= \frac{\sigma P_0}{(2\pi mkT)^{1/2}}(1 - \theta_{eq})^2 \exp\left(-\frac{E_a}{RT}\right)\\ &\quad - k_{-1}\theta_{eq}^2 \exp\left(-\frac{E_d}{RT}\right).\end{aligned} \tag{14}$$

By comparing Eqs. (10) and (14), k_f and k_b are given by (*11*)

$$k_f = \frac{\sigma}{(2\pi mkT)^{1/2}} \exp\left(-\frac{E_a}{RT}\right) \tag{15}$$

$$k_b = k_{-1} \exp\left(-\frac{E_d}{RT}\right). \tag{16}$$

Equations (11) and (15) lead to

$$\nu = \frac{\sigma(1 - \theta_{eq})^2}{(2\pi mk)^{1/2}T^{1/2}}(P_0 - P_{eq}) \exp\left(-\frac{E_a}{RT}\right). \tag{17}$$

Therefore, chemisorption rate $-dn_{H_2}/dt$ is given by

$$-\frac{dn_{H_2}}{dt} = K_0 \cdot \nu \cdot S/A = \frac{S\sigma(1-\theta_{eq})^2 K_0}{A(2\pi mk)^{1/2}} T^{-1/2}(P_0 - P_{eq}) \exp\left(-\frac{E_a}{RT}\right), \quad (18)$$

where n_{H_2} is the number of moles of hydrogen chemisorbed dissociatively, K_0 the number of absorption sites per unit area, S the total surface area of the activated particles of W grams of Mg_2Ni, and A Avogadro's number.

Equation (18) leads to

$$\frac{dF}{dt} = -\frac{M}{2W}\frac{dnH_2}{dt} = \frac{MS\,\sigma(1-\theta_{eq})^2 K_0}{2AW(2\pi mk)^{1/2}} T^{-1/2}(P_0 - P_{eq}) \exp\left(-\frac{E_a}{RT}\right), \quad (19)$$

where M is the molecular weight of Mg_2Ni.

Anderson and Baker (*16*) found that the isotherms of hydrogen at 90 K on evaporated nickel films were substantially flat in the region 10^{-4} to 10^{-3} Torr, which was taken to indicate that a monolayer had been completed.

Under $P_{eq} \geq 2.2$ bar and $548 \leq T \leq 593$ K, the experimental conditions of this work, it is considered that the flat portion in the isotherms of hydrogen chemisorbed on Ni or Mg_2Ni is reached at the starting point of the hydriding reaction, indicating completion of the monolayer. Thus, it can be considered that θ_{eq} is nearly independent of the experimental temperature.

So Eq. (19) can be rearranged as

$$\frac{dF}{dt} = CT^{-1/2}(P_0 - P_{eq}) \exp\left(-\frac{E_a}{RT}\right), \quad (20)$$

where

$$C = \frac{MS\,\sigma(1-\theta_{eq})^2 K_0}{2AW(2\pi mk)^{1/2}}$$

which is constant.

Equation (20) shows that, if the dissociative chemisorption of hydrogen on the metal surface is the rate-controlling step, the hydriding reaction rate dF/dt is a first-order function of $(P_0 - P_{eq})$ and depends on temperature by a function $f(T)$:

$$f(T) = CT^{-1/2} \exp\left(-\frac{E_a}{RT}\right). \quad (21)$$

The Arrhenius-type plot, $\ln[(dF/dt)T^{1/2}/(P_0 - P_{eq})]$ vs $1/T$, is shown in Fig. 7 by using the data of Table II and considering an increase temperature of 5 K. It corresponds to a relatively good linearity and gives a small and positive activation energy E_a of 220(cal/mole H_2), i.e., the dissociative chemisorption of hydrogen satisfies the requirements of case (ii).

Thus, the overall rate equation is given by

$$\frac{dF}{dt} = 1.634T^{-1/2}(P_0 - P_{eq}) \exp\left[-\frac{220(\text{cal/mole H}_2)}{RT}\right]. \quad (22)$$

In other words in the initial range ($\sim 0.05 < F < \sim 0.40$) of the hydriding reaction (Region II), the reacted fraction F at time t (min) is given by

$$F = F^* + 1.634T^{-1/2}(P_0 - P_{eq})(t - t^*) \exp\left[-\frac{220(\text{cal/mole H}_2)}{RT}\right].$$

The values of F^* and t^* are listed in Table II.

B. The Later Stage in the Hydriding Reaction (Region II)

The activated particles of Mg_2Ni have irregular shapes and various sizes as considered above.

While the hydriding reaction is complete in the smaller particles or in some sharp parts of the particles, resulting in the decrease of the unreacted fraction, the hydriding reaction is still taking place in some larger particles.

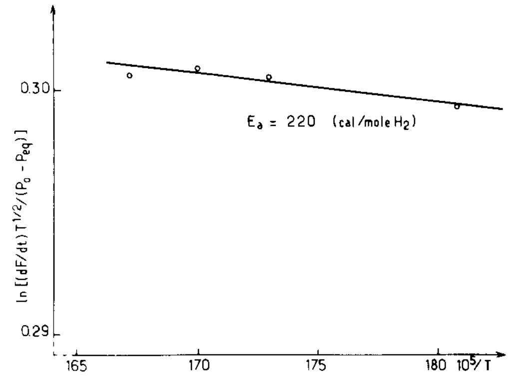

FIG. 7. Arrhenius-type plot of $\ln[(dF/dt)T^{1/2}/(P_0 - P_{eq})]$ vs $1/T$ by considering an increase in temperature of 5 K.

Thus, the overall hydriding reaction rates decrease gradually in this stage and finally the reaction reaches equilibrium.

Discussion

When the mean free path of hydrogen molecules ($\lambda = 3.32 \times 10^{-6}$ cm at 573 K, 7 bar) is smaller than the diameter ($2r$) of the pores of the filter or the interparticle channels or the cracks etc., the mass transport of H_2 molecules progresses by the forced flow and/or ordinary gas diffusion. When λ is larger than $2r$, the Knudsen or molecular diffusion occurs ((*19*), p. 212 in (*9*)).

Here, the average porosity (5 μm) of the stainless-steel filter used is larger than λ, resulting in a forced flow or ordinary gas diffusion. In the activated particles of Mg_2Ni there may be paths whose $2r$ values are larger or smaller than λ. From the viewpoint of the flux of hydrogen molecules arriving on the reaction surface, the three flows mentioned above therefore occur as parallel processes.

Thus the total flux of hydrogen is given by the sum of the flux of three flows, whose main part is given by the forced flow and the ordinary gas diffusion. This indicates that the Knudsen diffusion is not a rate-controlling step. The forced flow and the ordinary gas diffusion of hydrogen cannot likewise be considered as rate-controlling steps since they are faster than the diffusion of hydrogen through the solid phase (hydride layer).

If one compares the activation energies of diffusion on the surface (Qs) along the grain boundary (Qb) and within the lattice (Ql), $Q\text{s} < Q\text{b} < Q\text{l}$ (*20*). Turnbull, quoted by Chalmers (*21*), showed that D_b/D_l (representing the ratio of the diffusion coefficients for grain boundary and lattice) is $10^3 \sim 10^6$ according to the grain size. These trends can be applied to metal–H_2 system. These facts permits us to conclude that the surface diffusion of hydrogen atoms on the metal surface and the diffusion of hydrogen atoms through the grain boundary cannot be considered as the rate-controlling step.

According to Auer and Grabke (*22*), the activation energy for the transition of hydrogen atoms from the chemisorbed into the absorbed state is 6.8 kcal/mole for the Pd–H_2 system, which is much larger than that obtained here. But Flanagan (*9*) argued that the preexponential factor for this transition step should be larger than that for chemisorption. Thus, this step can also be eliminated as a rate controlling step.

In a steady-state experiment with a nominally fixed composition and with a fixed reaction surface area, if the reaction rate is independent of time ("linear rate law"), the interface chemical reaction (i.e., chemisorption or phase transformation) is most probably rate controlling. The F–t curves in Figs. 2 and 3 follow the linear rate law in the initial stage of the hydriding reaction where the reaction interface area is nearly constant. The pressure and temperature dependence of the results analyzed above show that chemisorption is the rate-controlling step. The low activation energy, about 220 cal/mole H_2, indicates that the phase transformation is not a rate-controlling step. Boser (*23*) reported that the activation energy for hydrogen absorption is 7.6 kcal/

mole H_2 and that the rate-controlling step for hydrogen absorption in $LaNi_5$ is the phase transformation. Our value is much lower than this reported data. Under the same limiting conditions, when diffusion is rate-controlling, a nonlinear time dependence usually results.

From the analysis of the results and the above discussion, one can conclude that the rate-controlling step is the dissociative chemisorption of hydrogen molecules, which involves heat transfer as "a rate-delaying step" and the low activation energy for the dissociative chemisorption E_a, suggests that Ni acts as the active site for the dissociative chemisorption of hydrogen molecules (*12, 24, 7*).

The history of the segregated Ni is different from that of the Ni in excess. The chemical affinity of Ni with O_2 is weaker than that of Mg. X-Ray diffraction analysis shows the presence of Mg oxide but not of nickel oxide in the starting material. Thus one may consider that the chemical states of the segregated Ni and the Ni in excess are the same, i.e., both Ni states act as the active sites for the dissociative chemisorption of hydrogen molecules.

The heat of chemisorption of hydrogen on Ni surface is reported to be about $-29 \sim -32$ (kcal/mole H_2) (*13*). The heat of formation of the Mg_2Ni hydride is about $-14.8 \sim -15.4$ (kcal/mole H_2) (*4, 2*). The large values of the exothermic heat of chemisorption and the heat of hydride formation are the cause of the increase in temperature in the course of reaction.

The reacted fractions at the S point for the F–t curves of 3 bar/548 K and 7 bar/593 K, which exhibits the incubation period, are reached as soon as hydrogen is charged, and scarcely change during the manipulation to obtain them. On the other hand, the reacted fractions at the S point of 7 bar/573 K and 7 bar/583 K represent the sum of the hydrogen absorbed as soon as the hydrogen is charged and the hydrogen absorbed during the manipulation to obtain them, which indicates the start of the hydriding reaction.

The compositions at the solubility limit of the α-phase were reported to be $Mg_2NiH_{0.27}$ and $Mg_2NiH_{0.3}$ according to the temperature (*25, 2*). Their compositions correspond to $F = 0.068$ and 0.075, respectively. The reacted fractions at the point S for 3 bar/548 K and 7 bar/593 K are lower ($F = \sim 0.053$, ~ 0.065) as compared with the reported solubility limit of the α-phase. This indicates that hydrogen is not saturated up to the solubility limit of the α-phase. Therefore we conclude that at the very beginning of the reaction, the extremely rapid absorption (Region I) is due to formation of a nonsaturated α-solid solution under the conditions of 3 bar/548 K and 7 bar/593 K, and due to the formation of a nonsaturated α-solid solution and a very small amount of surface hydride at 7 bar/573 K and 7 bar/583 K.

The appearance of the incubation period in the F–t curves at 3 bar/548 K and 7 bar/593 K is considered to result from a slow nucleation of the Mg_2Ni hydride under these conditions.

The F–t curve at 7 bar/548 K in Fig. 2 shows a slightly smaller reacted fraction after about 5 min than that of Fig. 3. They are the F–t curves of the 39th and 10th absorption cycles, respectively. This represents the influence of the number of absorption cycles. The hydrogen storage capacity of Mg_2Ni decreases along with the number of absorption cycles. The decomposition of Mg_2Ni into MgO and Ni by introduction of O_2 with absorption cycles can be considered as the reason for this phenomenon. However, there is a very small change in the F–t curves in the initial stage of the hydriding reaction.

Nomura *et al.* (*4*) and Akiba *et al.* (*5*) have studied the hydriding kinetics of this system by employing metal hydrides which had various H/Mg_2Ni ratios (n) to investigate the influence of composition of metal hydride on the hydriding reaction rates. They used a specially designed reaction vessel to obtain good heat transfer such as reported by Boser (*23*); in their work they observed a small increase in temperature of 1 ~ 1.6°C. However, they could not overcome the heat-transfer problem since they limited $P_0 - P_{eq}$ to about 1 bar, which limits the change in n to 0.1. The resulting decrease in the driving force for hydriding was 10 ~ 20% and even more in the later stage. On the assumption that the period of their initial stage (10^{-2} s) is constant at all temperatures, the equation for change in n (Eq. (4) in Ref. (*4*), Eq. (1) in Ref. (*5*)) can be considered as a rate equation in which the reaction rate is proportional to the driving force, and the rate constants show an inverse temperature dependence. These pressure and temperature dependences are in good agreement with our results, which indicates that the rate-controlling step is the chemisorption of hydrogen on the metal surface. In their later reaction stage the authors observed that the rate Eq. (5) of Ref. (*4*) or Eq. (2) of Ref. (*5*) can be integrated into a rate equation which obeys a "logarithmic law" and insisted that the rate-controlling step is the diffusion of the reactant through the very thin layer. They also reported that the reaction rates were not influenced by the ratios of H to Mg_2Ni. However, the independence of the reaction rates on the H/Mg_2Ni ratios n indicates that the rate-controlling step is a chemical reaction (chemisorption or phase transformation) rather than a diffusion process. If diffusion would be the rate-controlling step, the reaction rate would depend on n, since the diffusion distance increases with the increase of n, i.e., with the growth of the hydride layer.

In their later stage, because of the very small driving force for hydriding, they could not detect the influence of temperature (resulting in zero activation energy) and of the sudden pressure drop similar to that observed in their initial stage. In any event, their analysis shows, according to the reacted fraction, a set of discontinuous rate-controlling steps, i.e., a rate-controlling step related to the initial rapid process (I) → diffusion (II) → I → II · · ·. The fact that the equation of their initial stage can be applied up to $n = 3$ (corresponding to $F = 0.75$) shows that there is no reason for a change of the hydriding mechanism: hydride layers formed before their experimental conditions are not different kinetically from the thin hydride layer of their initial stage; this indicates that the rate-controlling step does not change in the later stage of the hydriding reaction.

Stucki (*6*) studied on the hydriding kinetics of the Mg_2Ni alloy. Under 10 bar H_2, the absorption kinetics was much faster at 480 K than at 580 K.

Conclusions

(1) In the hydriding process of Mg_2Ni, the rate-controlling step is the dissociative chemisorption of hydrogen molecules which involves heat transfer as "the rate-delaying step."

(2) The very small activation energy shows that the segregated and excess Ni are the active sites for the dissociative chemisorption.

(3) At the very beginning of the reaction, the extremely rapid absorption of hydrogen is due to formation of nonsaturated α-solid solution and a very small amount of surface hydride.

Acknowledgments

We thank Dr. J. P. Manaud for help with the experiments and Dr. J. P. Bonnet for the TEM investigation.

References

1. R. H. Wiswall, Jr. and J. J. Reilly, Jr., U.S. Pat. Office, 3,315,479 patented April 25, 1967.

2. J. J. Reilly and R. H. Wiswall, Jr., *Inorg. Chem.* **7,** 2254 (1968).
3. H. M. Lutz and O. De Pous, "Proceedings of the 2nd International Congress on Hydrogen in Metals," Pergamon, Oxford (1977).
4. K. Nomura, E. Akiba, and S. Ono, *Int. J. Hydrogen Energy* **6,** 295 (1981).
5. E. Akiba, K. Nomura, S. Ono, and S. Suda, *Int. J. Hydrogen Energy* **7,** 787 (1982).
6. F. Stucki, *Int. J. Hydrogen Energy* **8,** 49 (1983).
7. A. Seiler, L. Schlapbach, Th. Von Waldkirch, D. Shaltiel, and F. Stucki, *J. Less-Common Met.* **73,** 193 (1980).
8. L. Schlapbach, A. Seiler, F. Stucki, and H. C. Siegmann, *J. Less-Common Met.* **73,** 145 (1980).
9. T. B. Flanagan, "Proceedings, International Symposium on Hydrides for Energy Storage, Geilo," pp. 135–150, Pergamon, Oxford (1977).
10. P. S. Rudman, *J. Appl. Phys.* **50,** No. 11, 7195 (1979).
11. C. N. Park, Ph.D. thesis, Korean Advanced Institute of Science and Technology, 1982.
12. W. M. Mueller, J. P. Blackledge, and G. G. Libowitz, "Metal Hydrides," p. 53, Academic Press, New York/London (1968).
13. G. C. Bond, "Catalysis by Metals," Academic Press, p. 106, New York/London (1962).
14. J. W. Ward, *J. Less-Common Met.* **73,** 183 (1980).
15. O. Beeck, "Advances in Catalysis," Vol. 2. p. 151, Academic Press, New York (1950).
16. J. R. Anderson and B. G. Baker, *J. Phys. Chem.* **66,** 482 (1962).
17. K. J. Laidler, "Chemical Kinetics," p. 261, McGraw–Hill, New York (1965).
18. J. Szekely, J. W. Evans, and H. Y. Sohn, "Gas-Solid Reactions," p. 39, Academic Press, New York (1976).
19. J. M. Thomas and W. J. Thomas, "Introduction to Principles of Heterogeneous Catalysis," p. 34, Academic Press, New York/London (1967).
20. S. Z. Bokshtein, "Diffusion Processes, Structures, and Properties of Metals," p. 3, Consultants Bureau, New York (1965).
21. B. Chalmers, "Physical Metallurgy," Wiley, New York/London (1962).
22. W. Auer and H. J. Grabke, *Ber. Bunsenges. Bd.* **78,** 58 (1974).
23. O. Boser, *J. Less-Common Met.* **46,** 91 (1976).
24. H. C. Siegmann, L. Schlapbach, and C. R. Brundle, *Phys. Rev. Lett.* **40,** No. 14, 972 (1978).
25. M. H. Mintz, Z. Gavra, G. Kimmel, and Z. Hadari, *J. Less-Common Met.* **74,** 263 (1980).